Oxygen surface exchange kinetics of La 1– x Sr x CoO 3– δ thin-films decorated with binary oxides: links between acidity, strontium doping, and reaction kinetics

Alexandre Merieau, Matthäus Siebenhofer, Christin Böhme, Markus Kubicek, Olivier Joubert, Juergen Fleig, Clément Nicollet

Oxygen surface exchange kinetics of $La_{1-x}Sr_xCoO_{3-\delta}$ thin-films decorated with binary oxides: links between acidity, strontium doping, and reaction kinetics.

Alexandre Merieau[1], Matthäus Siebenhofer[2,3], Christin Böhme[2], Markus Kubicek[2], Olivier Joubert[1], Juergen Fleig[2], Clément Nicollet[1]

[1]Institut des Matériaux de Nantes Jean Rouxel (IMN), UMR6502 CNRS-Université de Nantes, Fédération de recherche Hydrogène

[2]TU Wien, Institute of Chemical Technologies and Analytics, Vienna, Austria

[3]Massachusetts Institute of Technology, Department of Nuclear Science and Engineering, 02141 Cambridge, USA

Recent studies showed that binary oxide modifications can induce substantial changes of the oxygen exchange kinetics at the surface of $Pr_{0.1}Ce_{0.9}O_{2-\delta}$ electrodes. The effect of these oxides was linked to their Smith acidity. In this work, these observations of oxides at the surface of mixed conducting oxides are extended to a metal-like conducting oxide: $La_{1-x}Sr_xCoO_{3-\delta}$. Samples of $La_{1-x}Sr_xCoO_{3-\delta}$ with various Sr content deposited by PLD were investigated in situ during the deposition process by impedance spectroscopy, before and after decoration with SrO, CaO and SnO_2 at different temperatures and pO_2. Considering experimental observations from the literature, the kinetics of decorated surfaces follow the Smith acidity of the binary oxide, which confirms that this scale is a good descriptor for sorting impurities. No notable effects of the Sr content on the decoration impact were measured and the effect of impurities was compared between $La_{1-x}Sr_xCoO_{3-\delta}$ and $Pr_{0.1}Ce_{0.9}O_{2-\delta}$ from a previous study. Basic impurities added at the surface of $La_{1-x}Sr_xCoO_{3-\delta}$ electrodes showed less influence on the reaction kinetics than on $Pr_{0.1}Ce_{0.9}O_{2-\delta}$, but a stronger impact was found with acidic oxides. This effect is supposed to originate from the acidity difference that controls a major part of the oxygen exchange kinetics. These results underline that the outermost surface is decisive for solid oxide cell electrode materials and that the relative insensitivity of the kinetics to bulk properties might lead to a high flexibility in terms of electrode design and material combination.

1 Introduction

The oxygen exchange reaction in mixed conducting oxides is a critical process in solid oxide fuel cells (SOFCs), where oxygen is reduced to form oxide ions at the cathode. The oxygen exchange reaction can be written in Kröger-Vink notation as

$$2e' + v_O^{\cdot\cdot} + \frac{1}{2}O_2 \leftrightarrow O_O^X, \qquad 1$$

which involves electrons e', oxygen vacancies $v_O^{\cdot\cdot}$, molecular oxygen O_2 and lattice oxygen O_O^X. The rate at which oxygen exchange occurs is directly dependent on the availability of the reactants. These reactants concentrations are influenced by numerous factors, including intrinsic physical properties of the mixed conducting oxides and operating parameters, such as temperature or pO_2.

The most broadly accepted parameters to accelerate oxygen exchange kinetics are the concentration and mobility of oxygen vacancies of the mixed conducting oxide surface. Indeed, Kilner and De Souza[1] showed a correlation between the oxide ion diffusion coefficient and the oxygen exchange kinetics, which holds for a wide range of mixed conducting oxides. For perovskite-type oxides such as $LaCoO_3$, the oxygen transport properties can be controlled by tuning the concentration of acceptor dopant on the A site, which modifies the concentration of charged defects, such as oxygen vacancies or electron holes. However, it can be argued that simply relying on transport properties for describing oxygen surface

exchange kinetics is incomplete. This can be exemplified by the wide scattering of surface exchange coefficients measured on nominally identical compositions[2]. Those discrepancies point towards important effects of surface chemistry and surface electronic properties on the oxygen exchange kinetics in mixed conducting oxides. For example, Tripkovic *et al.*[3] showed that changes of oxygen exchange kinetics were linked to the aging of the electrode surface between 700 °C and 800 °C. It was suggested that at these temperatures the surface is enriched in Sr, inducing a sensitivity increase to pollutants such as S, Cr, CO_2 and H_2O[4–7]. In two recent studies, it has been shown that surface modifications have a huge importance in controlling oxygen exchange kinetics in Pr-doped ceria, and that their effect can be correlated to their acidity[8,9].

However, the extrapolation of these conclusions to other mixed conducting oxides is not straightforward, and should be studied thoroughly. Indeed, from Nicollet *et al.*[8], the main hypothesis to explain the role of impurities on surface exchange kinetics is a change of work function of the surface of the mixed conducting oxide, which in turn changes the availability of charge carriers for the oxygen exchange reaction.

Pr-doped ceria is a mixed conducting[10] oxide showing a n-type conduction for a temperature superior to 600 °C and oxygen partial pressure between 1 and 10^{-6} atm. In this structure, the conduction of the electronic charges occurs by polaron hopping from Pr^{3+} to Pr^{4+}. It is the presence of Pr on Ce site that induces the formation of an impurity band allowing the polaron hopping. On the other hand, the oxide ions are conducted through the oxygen vacancies formed to compensate formation of electron by reduction of Pr^{4+} into Pr^{3+}. At 650 °C and a partial pressure of oxygen of 10^{-2} atm, the material shows a conductivity of 3.10^{-2} $S{\cdot}cm^{-1}$ with a transference number close to 0.4 inducing an ionic conductivity close to the electronic conductivity. Considering these observations from the literature, it can be argued that those changes in the surface electronic structure are important to the oxygen exchange reaction because the conduction band electron concentration is initially low (and there is more room for variation).

Then, it is necessary to measure whether the same effects can be observed with impurities on mixed conductors with higher electronic conductivity, such as $La_{1-x}Sr_xCoO_{3-\delta}$, which exhibits metal-like conductivity due to the overlapping of the oxygen 2p band and cobalt 3d band[11,12]. This material exhibit a conduction of oxygen through vacancies mainly induced by donor doping with Sr on La sites. As a matter of comparison with Pr-doped ceria, $La_{0.6}Sr_{0.4}CoO_{3-\delta}$[13] presents an ionic conductivity close to 5.10^{-3} $S.cm^{-1}$ at 650°C and a total conductivity of 2000 $S.cm^{-1}$ at 10^{-2} atm of pO_2 partial pressure. The main changes with $La_{0.6}Sr_{0.4}CoO_{3-\delta}$ would then be the modification of the electrode surface acidity due to the composition and the electronic conduction properties.

In a recent publication, Siebenhofer *et al.*[14] showed the improving capabilities of small amounts of SrO on $La_{0.6}Sr_{0.4}CoO_{3-\delta}$ surfaces at high temperatures (600 °C). At lower temperatures, the deposited SrO reacted with CO_2 traces from the surrounding atmosphere, forming $SrCO_3$ and leading to performance degradation. With these results, they further substantiated the importance of the Smith acidity scale as a tool to understand the effect of impurities on oxygen electrodes. Acidic CO_2 may counterbalance the enhancement induced by the basic SrO decoration.

In this work, we studied the surface exchange kinetics by systematic impurity decoration of mixed conducting oxides, while modifying the transport properties of the host material through a variation of the acceptor doping concentration. $La_{1-x}Sr_xCoO_{3-\delta}$ with varying Sr content was decorated with acidic and basic impurity oxides. An i-PLD setup[15] was used to measure the oxygen surface exchange coefficient of $La_{1-x}Sr_xCoO_{3-\delta}$ films *in situ*, during the deposition and decoration procedures (inside the PLD chamber)[15], allowing for measurements in exceptionally clean conditions and on pristine surfaces. By changing the strontium doping concentration of the electrode, the effect of surface decorations is investigated depending on the electronic structure of the host material, and the limits of the applicability of the Smith acidity are explored.

2 Experimental

2.1 Targets preparation

$La_{1-x}Sr_xCoO_{3-\delta}$ targets with three strontium concentrations were synthesized, namely 5, 10 and 20 at. % of strontium on the perovskite A-site. The $La_{1-x}Sr_xCoO_{3-\delta}$ powders used for the targets for the pulsed laser deposition were prepared by a glycine nitrate combustion route with a fuel-nitrate ratio of 1.2 using metal nitrates as reactants (Sigma-Aldrich: $SrNO_3$ > 99 %, $La(NO_3)_3 . 6H_2O$ 99.995 %, and $Co(NO_3)_3 . 6H_2O$ > 98 %). The nitrates and glycine were dissolved in pure mili-Q water (18.2 MΩ.cm) and the mixture was dehydrated on a hot plate at 120°C overnight and heated at 300°C to trigger the combustion reaction. The ashes from the synthesis were annealed at 1000 °C for 3 h in air to obtain the pure perovskite phase (controlled by X-ray diffraction, see Supplementary Note 1). Then, the powder was pressed into a 30 mm pellet under 56 MPa uniaxial pressure and sintered at 1300 °C for 10 h in air. The relative density of the target was above 90 % for all three compositions.

The composition of the targets was controlled by inductively coupled plasma atomic emission spectroscopy (ICP-AES) using an ICP spectrometer ThermoScientific iCAP 6000 Series. The pellet was dissolved in HNO_3 10 % and analysed by the standard addition method. The stoichiometries obtained for the various $La_{1-x}Sr_xCoO_{3-\delta}$ targets are $La_{0.95}Sr_{0.05}Co_{1.00}O_{3-\delta}$, $La_{0.90}Sr_{0.10}Co_{1.00}O_{3-\delta,}$ and $La_{0.80}Sr_{0.20}Co_{1.00}O_{3-\delta}$. The uncertainty associated to the ratio of the cations is ≈ 0.01 for all compositions (see Supplementary Note 2).

For the decoration of the $La_{1-x}Sr_xCoO_{3-\delta}$ thin film electrodes, targets of the respective binary oxides (SrO, CaO, SnO_2) were prepared from the respective calcined powders (Sigma-Aldrich, > 99.9 %) by isostatic pressing and sintering. Basic oxides had to be calcined before pressing (12 h at 1200 °C in O_2 flow) to decompose hydroxides and carbonates formed by reaction with ambient air. To avoid hydration or carbonation of the oxides after sintering, the targets were stored in a desiccator with a drying agent (silica gel) under vacuum. For the selection of decorated oxides, several factors were considered: the band gap energy (it should be smaller than the laser energy), Smith acidity, and the potential pollution of the setup. Three oxides were selected: SnO_2, SrO, and CaO; SnO_2 being one of the most acidic (2.2), CaO (-7.5), and SrO being among the most basic that can be deposited (-9.4).

2.2 Cell preparation

First, current collector grids (Ti/Pt, 5/300 nm, 20 μm square holes/5 μm stripes) were prepared by lift-off photolithography and metal sputtering (BalTec MED 020, Leica Microsystems GmbH, Germany) on both sides of (100) oriented yttria stabilized zirconia (YSZ, 9.5 mol.% Y_2O_3, Crystec GmbH, Germany) single crystalline substrates ($5 \times 5 \times 0.5$ mm^3). These grids served as the base for working electrode (WE) and counter electrode (CE). All depositions were done with a KrF (λ = 248 nm) excimer laser (Lambda Physics, COMPex Pro 201) with a laser fluence of approximately 1.17 J cm^{-2} at the target at a target/sample distance of 6 cm. Before every i-PLD measurement, the deposition rate of each decoration target was determined with a quartz microbalance inside the PLD chamber at 0.04 mbar O_2 and room temperature.

On the working electrode side of the YSZ substrate, a 5 nm thick $Gd_{0.2}Ce_{0.8}O_{2-\delta}$ (CGO) buffer layer was deposited by PLD on top of the current collector grids with 90 laser pulses at a frequency of 2 Hz at 600 °C (measured with a pyrometer (Heitronics)) and 0.04 mbar of O_2. This buffer layer avoided interfacial reactions of the electrode and YSZ and warrants (001) oriented growth of $La_{1-x}Sr_xCoO_{3-\delta}$[17]. For the counter electrode, the target to substrate distance was set to 5 cm, the atmosphere was set to 0.4 mbar pO_2 and the substrate was heated to a temperature of 450 °C. 9000 laser pulses at a frequency of 5 Hz were shot on a $La_{0.6}Sr_{0.4}CoO_{3-\delta}$ target, which produced a nanoporous, thick electrode[18].

2.3 Measurement protocol

To investigate the impact of oxide decoration on the oxygen surface exchange coefficient of the different compositions of $La_{1-x}Sr_xCoO_{3-\delta}$, a detailed measurement procedure was followed. This protocol is summarized in Figure 1. The deposition/measurement procedure was performed entirely within the vacuum chamber of the i-PLD setup, without exposition of the sample to the ambient atmosphere. The polarization resistance of the working electrode was measured at 600 °C and an oxygen pressure of 0.04 mbar. First, a 40 nm layer of $La_{1-x}Sr_xCoO_{3-\delta}$ was deposited, which is sufficient to ensure negligible in-plane resistance of the film. Then, the surface resistance of the $La_{1-x}Sr_xCoO_{3-\delta}$ thin film, associated to its oxygen exchange kinetics, was measured by impedance spectroscopy with an Alpha-A High Performance Frequency Analyzer and Electrochemical Test Station POT/GAL 30V/2A setup (Novocontrol Technologies) in the frequency range from 10^6 to 0.1 Hz, with a resolution of 5 points per decade and an AC amplitude of 10 mV RMS.

The temperature and pO_2 dependence of the pristine sample were measured following the sequence illustrated in Figure 1. The measurements were recorded at constant pO_2 of 0.04 mbar, between 600 °C and 500 °C for the temperature dependence, and at constant T = 600 °C between 10^{-5} and 10^{-1} bar for the pO_2 dependence.

The temperature during the measurement was controlled by tracking the ohmic offset of impedance curves, which includes the well-known ionic conductivity of the YSZ electrolyte[19], as well as wiring and grid contributions which were determined separately prior to measurements. The protocol associated to the temperature determination of the sample is developed in a previous article[20]. The temperatures presented in this articles are the temperature obtained from this protocol. The pristine sample was decorated with the selected oxide thin-film and the same measurement protocol is followed. From previous experiments the decoration process was verified using low energy ion scattering (LEIS), atomic force microscopy (AFM) and secondary ion mass spectrometry (SIMS) measurements[9,21,22]. These experiments showed a homogeneous decoration as well as a full coverage of the surface. Upon completion of the measurements with one decoration, the surface of the cell was regenerated with a $La_{1-x}Sr_xCoO_{3-\delta}$ deposition (to bury the decoration and eliminate its influence for subsequent decorations) and the next decoration is measured on a freshly deposited $La_{1-x}Sr_xCoO_{3-\delta}$.This protocol allows studying several decorations without the need of preparing a new cell, thus warranting minimal deviations due to sample preparation. The order of the measurement for each sample is first pristine, then SnO_2 decorated, CaO decorated and finally SrO decorated. Impedance curves show two dominating semicircles, an inductive contribution and a small interfacial high-frequency feature (see Fig. 1 b). The impedance was modelled using an equivalent circuit of three parallel R-CPE circuits connected in series, a resistance and an induction contribution at high frequency. The resistance associated to oxygen surface exchange on the growing electrode is extracted from the larger R-CPE contribution, the smaller feature at lower frequencies being associated to the counter electrode (due to the larger thickness and the larger chemical capacitance, the characteristic frequency of the counter electrode feature is significantly lower). The oxygen exchange kinetics was then derived from the resistance using Equation 2 proposed by Maier[23].

$$k^q = \frac{k_B T}{4e^2 R_{surf} c_o} \qquad 2$$

k^q is the electrical surface exchange coefficient of oxygen, k_B the Boltzmann constant, T the temperature, e the elementary charge, R_{surf} the measured surface resistance and c_O the oxygen concentration in the crystal lattice which was determined taking into account the vacancies concentration: $c_O = 5.074\times10^{22}$ cm^{-3}, $c_O = 5.117\times10^{22}$ cm^{-3}, $c_O = 5.139\times10^{22}$ cm^{-3} for $La_{0.8}Sr_{0.2}CoO_{3-\delta}$, $La_{0.9}Sr_{0.1}CoO_{3-\delta}$ and $La_{0.95}Sr_{0.05}CoO_{3-\delta}$, respectively. Considering the work of Kawada et *al.*, the concentration of oxygen change with the temperature and the pO_2, the variation is negligible *vs.* the impact of the donor doping of the material with a variation of the oxygen content respectively of a maximum of 0.03 % of c_O (see Supplementary Note 3)[24,25].

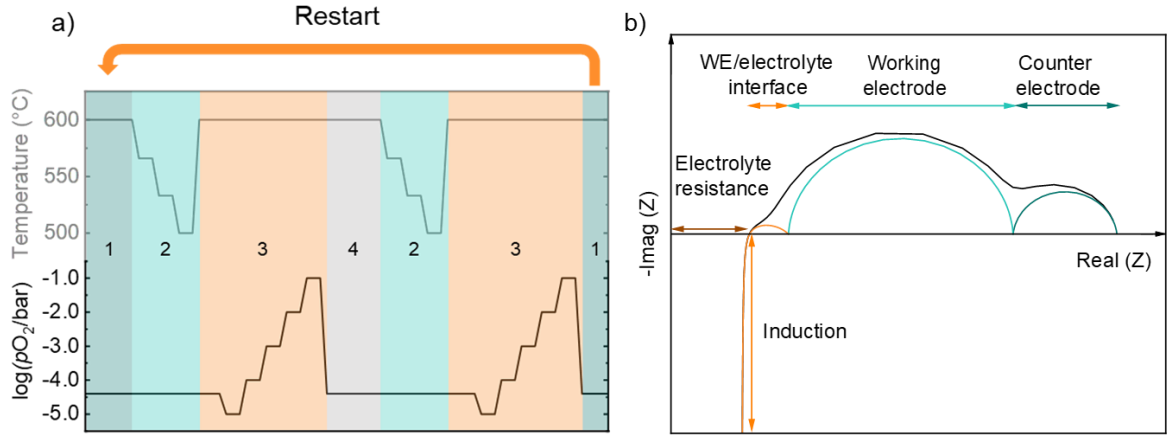

Figure 1 . a) Summary diagram of the i-PLD deposition and measurement protocol with 1.) deposition of $La_{1-x}Sr_xCoO_{3-\delta}$ thin-film/ $La_{1-x}Sr_xCoO_{3-\delta}$ regeneration, 2.) temperature dependence, 3.) pO_2 dependence and 4.) acid-base decoration, b) Illustration of a typical impedance diagram measured on $La_{1-x}Sr_xCoO_{3-\delta}$ /CGO/YSZ/porous $La_{0.6}Sr_{0.4}CoO_{3-\delta}$ cells.

3 Results

For each strontium content x in $La_{1-x}Sr_xCoO_{3-\delta}$, the dependence of the oxygen surface exchange coefficient with the thickness of the decorating binary oxide was studied. Then, the temperature and pO_2 dependence of the oxygen exchange coefficient was studied and compared for all Sr contents and decorations.

3.1 Influence of the decoration thickness and acidity on k^q

The influence of the decoration on the oxygen exchange kinetics is represented in Figure 2. The variation of the oxygen surface exchange coefficient is plotted for each $La_{1-x}Sr_xCoO_{3-\delta}$ composition and decoration. The error bars of the k value represented in the different Figures correspond to the standard deviation from pristine samples of $La_{0.6}Sr_{0.4}CoO_{3-\delta}$ calculated from previous studies detail in Supplementary information 4.

The initial surface exchange coefficients k^q for the three pristine samples is represented in Figure 2 a) with 1 post-$La_{1-x}Sr_xCoO_{3-\delta}$ decoration (before pO_2 and T dependence measurement). The general evolution of k^q follows the Sr content of the material with $La_{0.8}Sr_{0.2}CoO_{3-\delta}$ faster than $La_{0.9}Sr_{0.1}CoO_{3-\delta}$ faster than $La_{0.95}Sr_{0.05}CoO_{3-\delta}$. This evolution is in agreement with the trend proposed by Kilner *et al.*[1,26] that shows a direct relationship between dopant content and ionic conductivity. Fig. 2 a) also shows $La_{0.9}Sr_{0.1}CoO_{3-\delta}$ before SrO decoration as an outlier with a k^q value higher than expected from the observed trend with Sr content and a non-regenerated surface faster than regenerated ones. This evolution can be explained by a potential loss of preferential orientation of the thin-film impacting the oxygen exchange kinetics[27].

The decoration with CaO decreases the oxygen exchange kinetics by a factor 2.0 *vs* the pristine sample for $La_{0.9}Sr_{0.1}CoO_{3-\delta}$ and $La_{0.8}Sr_{0.2}CoO_{3-\delta}$ for 0.66 nm deposited, and by a factor 2.6 for $La_{0.95}Sr_{0.05}CoO_{3-\delta}$ for 0.53 nm deposited. In the case of CaO, it was predicted from previous work that the high basicity of this oxide should increase the oxygen exchange kinetics. Here the opposite effect is observed, which is commented in the discussion section of this article. SnO_2 decoration decreases the oxygen exchange coefficient k^q by a factor of 15, 10 and 10 *vs*. the pristine sample for 0.56 nm deposited on $La_{0.8}Sr_{0.2}CoO_{3-\delta}$, $La_{0.9}Sr_{0.1}CoO_{3-\delta}$ and $La_{0.95}Sr_{0.05}CoO_{3-\delta}$ respectively. The decoration with SrO produces an alternative behaviour. The oxygen surface exchange kinetics are initially enhanced with the SrO decoration, up to a factor 2 for 0.28 nm of SrO. The effect is observable regardless of the Sr content of the $La_{1-x}Sr_xCoO_{3-\delta}$ film. However, a turnover can be observed above this thickness for all three $La_{1-x}Sr_xCoO_{3-\delta}$ compositions. Interestingly, the decrease of k^q with the SrO loading changes similarly between the different nominal compositions of $La_{1-x}Sr_xCoO_{3-\delta}$.

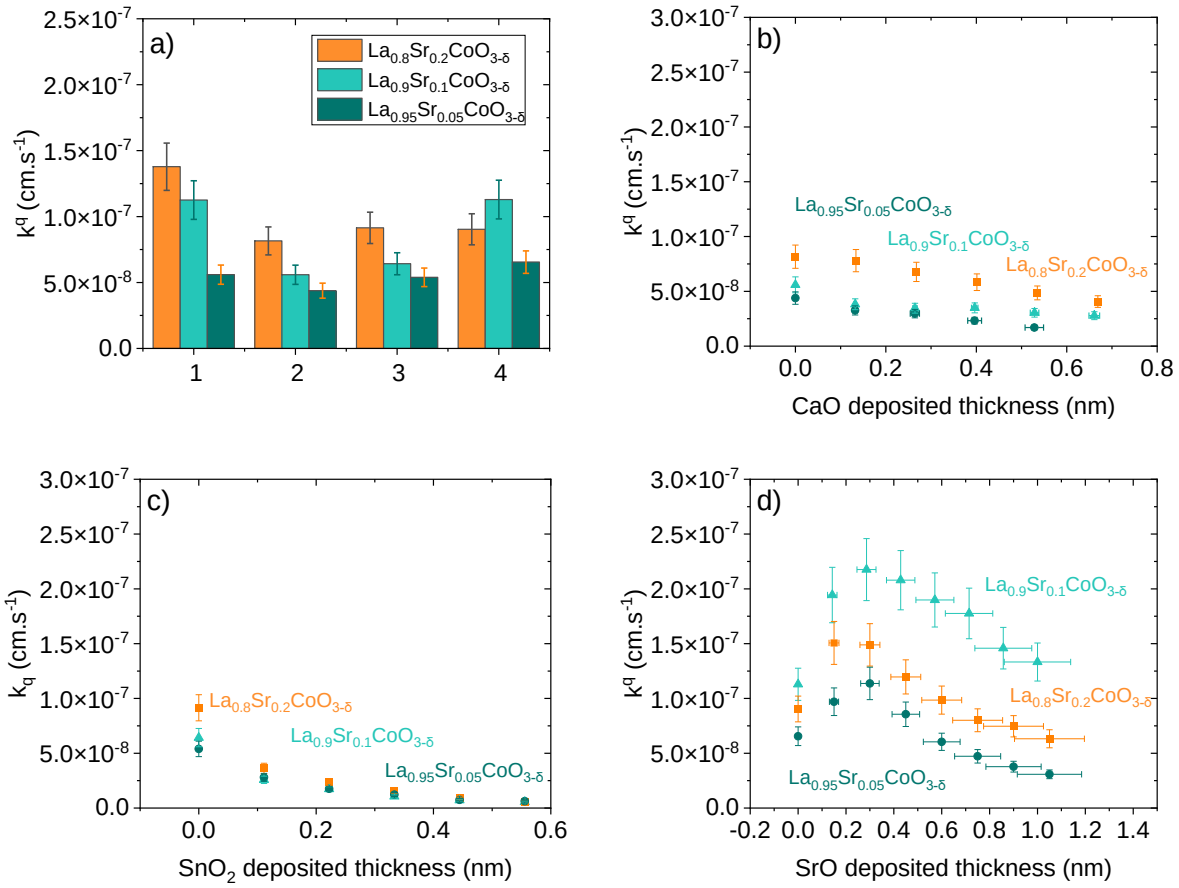

Figure 2. a) Initial oxygen surface exchange coefficients for pristine surfaces 1.) post-$La_{1-x}Sr_xCoO_{3-\delta}$ deposition, 2.) pre-CaO decoration, 3.) pre-SnO_2 decoration and 4.) pre-SrO decoration, k^q values as a function of the thickness of the decoration for b) CaO decoration, c) SnO_2 decoration and d) SrO decoration, $La_{0.95}Sr_{0.05}CoO_{3-\delta}$ *(●),* $La_{0.9}Sr_{0.1}CoO_{3-\delta}$ *(▲),* $La_{0.8}Sr_{0.2}CoO_{3-\delta}$ *(■) at 600 °C and 0.04 mbar of oxygen. The represented error bars correspond to the dispersion of k^q values from the measurement setup and the dispersion of the deposited oxide thickness values determined from the calibration process of the deposition process.*

3.2 pO_2 dependence

Prior to each surface regeneration, the oxygen dependence of the oxygen surface exchange coefficient for both pristine and decorated electrodes was determined. The surface exchange resistance was measured *in situ* within the vacuum chamber of the pulsed laser deposition system at 600 °C, with oxygen pressure ranging from 10^{-5} to 10^{-1} bar. The results are presented in Figure 3. The pristine $La_{1-x}Sr_xCoO_{3-\delta}$ exhibits two distinct pO_2 dependences at low pO_2 (< 10^{-3} bar) and high pO_2 (≥ 10^{-3} bar) with slope values of 0.52 ± 0.02 for low pressures and then a flatter dependence above 10^{-3} mbar pO_2. The general evolution matches the observation of a previous study by Siebenhofer *et al.*[15]. Here, the rate-limiting step of the reaction at low pO_2 involves molecular oxygen, while the lower slope at high pO_2 might be induced by degradation of the $La_{1-x}Sr_xCoO_{3-\delta}$ surface or a change of the rate-limiting step[15,24].

The pO_2 dependences were also recorded after each decoration (at the final thickness). Figure 3b), c) and d) show the pO_2 dependences of k^q after decorations with CaO, SnO_2 and SrO, respectively. No clear change of the slopes is observed with decorations, regardless of their Smith acidity, with low pO_2 slope values of 0.47 ± 0.02 for SnO_2 decorations, 0.49 ± 0.04 for SrO decorations and 0.50 ± 0.06 for CaO decorations. This suggests that the decorations do not fundamentally change the reaction path or the rate-determining step of the oxygen exchange reaction. It is again worth mentioning that the k^q values for the SrO decorated $La_{0.9}Sr_{0.1}O_{3-\delta}$ are higher than expected and undergo substantial degradation at higher pO_2.

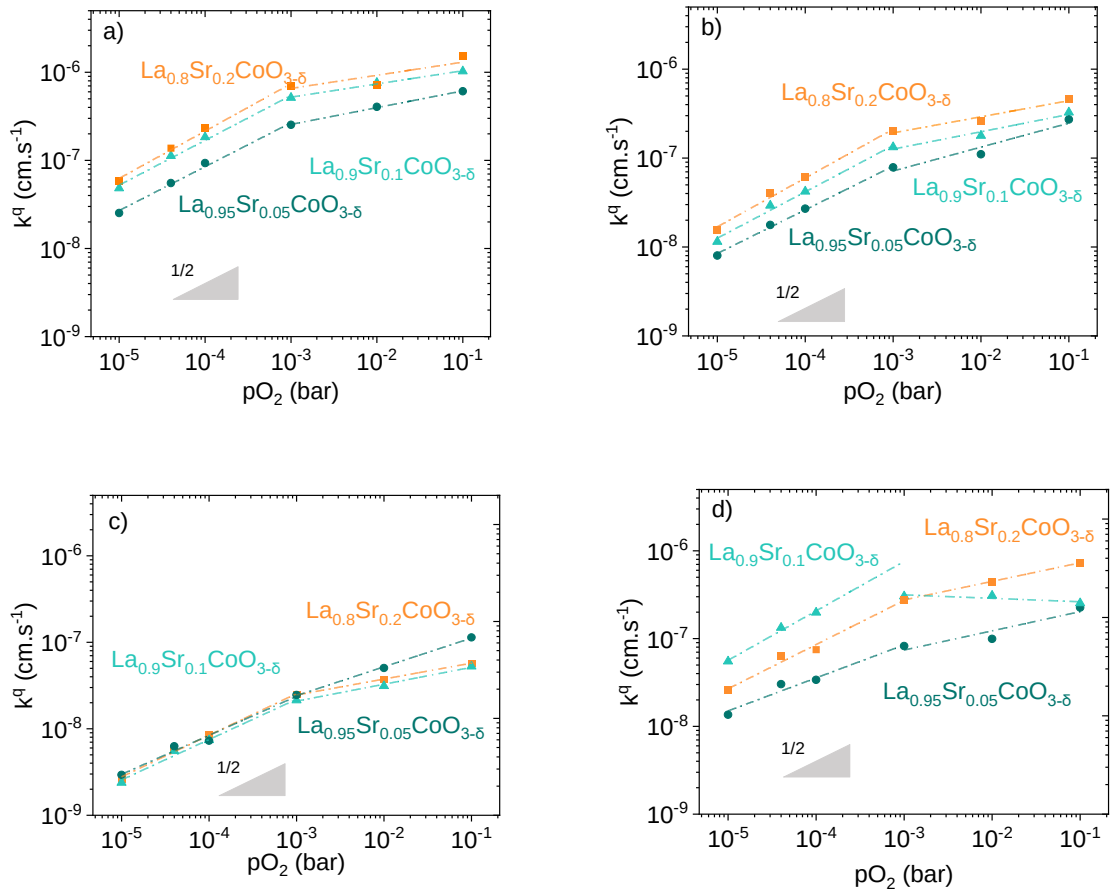

Figure 3. Oxygen partial pressure dependence of the oxygen surface exchange kinetics measured at 600 °C on a) pristine sample, b) CaO decorated sample, c) SnO_2 decorated sample and d) SrO decorated sample on $La_{0.8}Sr_{0.2}CoO_{3-\delta}$ (■), $La_{0.9}Sr_{0.1}CoO_{3-\delta}$ (▲) and $La_{0.95}Sr_{0.05}CoO_{3-\delta}$ (●).

3.3 Temperature dependence

Despite the decoration, it appears that the rate-determining step remains globally unchanged. To further study the mechanistic implications of the acid-base decorations, the temperature dependence of the surface exchange coefficient k^q was measured and compared between all decorations. The temperature dependences of k^q for all samples are presented as Arrhenius plots in Figure 4. The measurements are performed at the maximum loading for each decoration studied.

The activation energy of the oxygen exchange coefficient of $La_{1-x}Sr_xCoO_{3-\delta}$ seems to be more affected by SrO and CaO deposition than by SnO_2. The latter changes the activation energy from 1.28 eV for pristine $La_{0.8}Sr_{0.2}CoO_{3-\delta}$ to 1.35 eV, while for $La_{0.9}Sr_{0.1}CoO_{3-\delta}$, an increase in the activation energy from 1.26 to 1.50 eV was observed. On the other hand, CaO and SrO decorations increase the activation energy of the reaction dramatically with a smaller contribution for SnO_2 decoration: + 0.50 eV for CaO and up to + 0.89 eV for SrO and +0.16 eV for SnO_2. Those are the mean change value compared to the pristine sample for the different $La_{1-x}Sr_xCoO_{3-\delta}$. It is also worth emphasizing that the final decoration layer thickness of SrO is above 1 nm, which needs to be considered and is further discussed below. As a matter of comparison, the general variation observed on previously studied $Pr_{0.1}Ce_{0.9}O_{2-\delta}$ pristine samples[9] were about 0.1 eV for similar experimental conditions and similar regeneration process. In this study the dispersion for the decorations are higher, up to 0.25 eV for CaO decoration. This uncertainty can be associated to the thickness uncertainty of the decorations. Then, no conclusion can be made for the influence of SnO_2 decorations on the activation energies, since they are below the error bars. However, the variation observed with CaO and SrO decorations are significant and can be attributed to an effect of the decoration added at the surface. From these results it is clear that the decoration with

higher deposition content have an impact on the activation energy of the reaction in contrast to the previous study that showed negligible to no variation[8,9] over small quantity deposited using PLD.

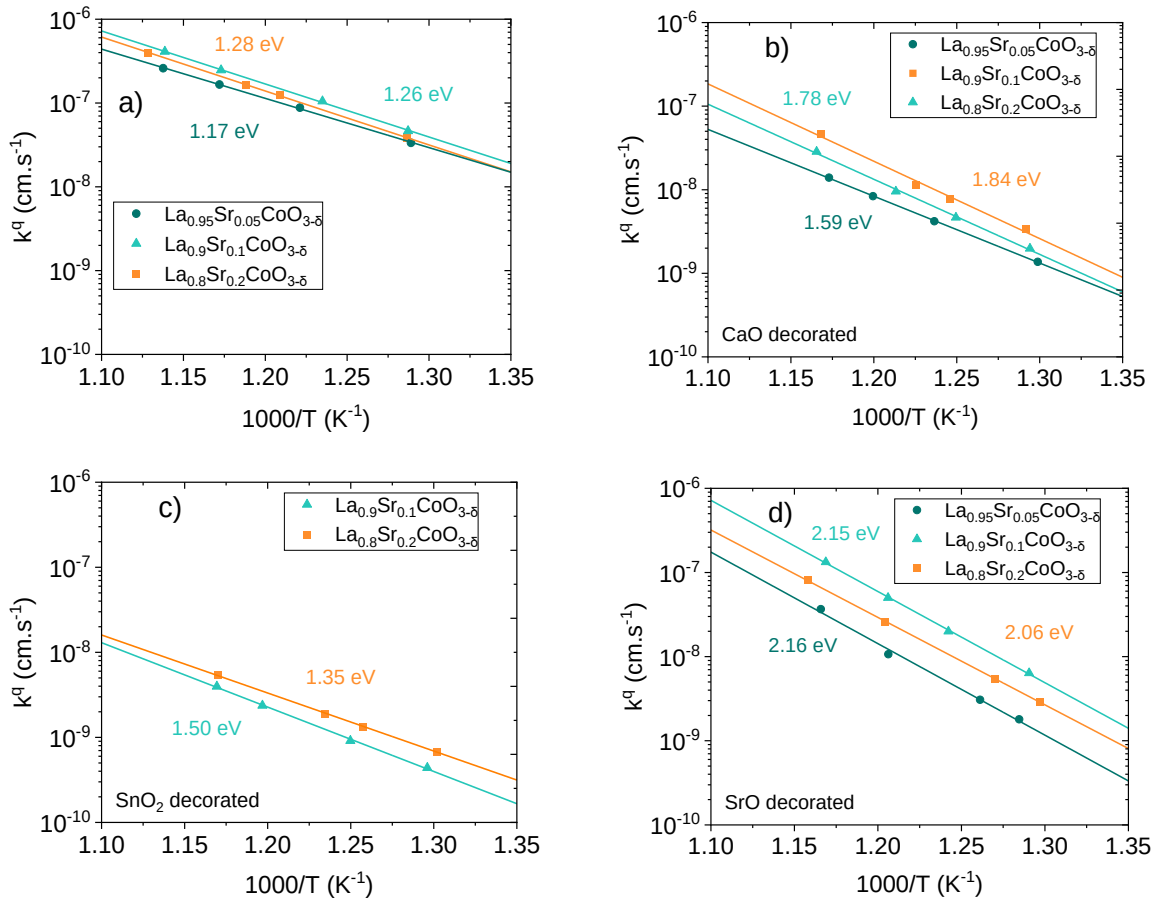

Figure 4. Temperature dependence of the oxygen surface exchange kinetics on a) pristine, b) CaO decorated, c) SnO_2 decorated d) SrO decorated surface of $La_{0.8}Sr_{0.2}CoO_{3-\delta}$ (■), $La_{0.9}Sr_{0.1}CoO_{3-\delta}$ (▲) and $La_{0.95}Sr_{0.05}CoO_{3-\delta}$ (●) at 0.04 mbar of O_2.

4 Discussion

In general, and as observed previously on Pr-doped ceria[8,9], the variation of k^q as a function of the decoration follows the Smith acidity scale, *i.e.* k^q decreases when the Smith acidity of the decoration increases. However, the decorations are mostly detrimental in the case of $La_{1-x}Sr_xCoO_{3-\delta}$, the only exception being found for small amount of SrO at 600°C. This discussion focuses on the surface resistance/oxygen exchange kinetics changes of the oxygen electrode upon decoration and with changing temperature and pO_2. The main focus of the discussion is the link between bulk properties of the material and the decoration effect.

4.1 Discussion on bulk *vs.* surface acidity

Based on the article of Nicollet and Tuller[28], it is possible to determine an equivalent Smith acidity for perovskite oxides with a general formula $A_xA'_{1-x}B_yB'_{1-y}O_{3-\delta}$ with Equation 3, which can be applied to nominal $La_{1-x}Sr_xCoO_{3-\delta}$ with various Sr contents.

$$\alpha_{A_xA'_{1-x}B_yB'_{1-y}O_3} = \frac{x\alpha_{AO} + (1-x)\alpha_{A'O} + y\alpha_{BO} + (1-y)\alpha_{B'O}}{2}. \qquad 3$$

In Equation 3, x denotes the A content, $(1-x)$ the A'content, y the B content and $(1-y)$ the B' content and α the acidity of the oxide associated to A, A', B and B'.

Using Equation 3, the acidity is -4.06, -3.74 and -3.58 for $La_{0.8}Sr_{0.2}CoO_{3-\delta}$, $La_{0.9}Sr_{0.1}CoO_{3-\delta}$, and $La_{0.95}Sr_{0.05}CoO_{3-\delta}$, respectively. From the point of view of the Smith acidity, the deposited CaO (-7.5) should enhance the oxygen exchange kinetics, but the opposite effect is observed. To better represent the 'true' acidity of the surface, observations from the literature have to be taken into account. Observations from literature have to be taken into account which suggest that the surfaces of $La_{1-x}Sr_xCoO_{3-\delta}$ perovskites are largely stabilized with an AO termination[11,29–32]. Then, the acidity of the surface would mainly be controlled by A site acidity, meaning a lower acidity than that of the bulk (A cations being more basic than B cations). Moreover, there is a large body of evidence that confirms the segregation of the acceptor dopant (here strontium) to the surface, thereby further decreasing the surface acidity[3,4,33,34]. These results are in agreement with Rupp *et al.*[16]: Using LEIS, they observed an enrichment of the surface in SrO (-9.4) up to 81 % after PLD of $La_{0.6}Sr_{0.4}CoO_{3-\delta}$. Considering these experimental observations the surface would then show an acidity closer from SrO acidity (-9.4), which would explain the detrimental effect of CaO decoration (-7.5).

With strontium decorations, the optimum in oxygen exchange kinetics is reached at approximately 0.273 nm deposited[35] which in monolayers corresponds to approximately one monolayer of SrO. From the pristine state to one monolayer of SrO, the suggested explanation for the increase of k^q is that further increasing Sr enrichment at the surface still decreases the Smith acidity, yielding an even more basic surface. Above one monolayer, the degradation of oxygen exchange kinetics for the three compositions suggest that the decoration blocks either one of the reactant species, *e.g.* electrons or oxygen vacancies. As the pO_2 dependence does not change with decoration, the rate-determining step should remain the same. However, the substantial changes of activation energy with decoration suggest that the energy barrier for the rate-limiting step is strongly affected by the type and amount of decoration. From this study, the mechanism causing this change of energy barrier remains unclear and will require a more in-depth analysis.

4.2 Discussion on the magnitude of the decoration effect

A second effect that requires discussion is the magnitude of the changes of k^q upon decoration with binary oxides. More precisely, how this magnitude varies depending on the starting mixed conducting oxide.

First, the relative change of ASR of various $La_{1-x}Sr_xCoO_{3-\delta}$ compositions is studied in relation to their dependency on the Smith acidity of the decoration, as illustrated in Figure 5 a). The relative change of ASR is calculated using the area specific resistance (ASR) at 1.5 monolayers of decoration normalized by the ASR of the pristine sample for the different $La_{1-x}Sr_xCoO_{3-\delta}$ compositions. The equivalent in terms of monolayers deposited is determined using the data available in Table 1.

Material	Parameter considered (nm)	Thickness of one monolayer (nm)	Monolayers deposited (comparison PCO/LSC)
CaO	0.486	0.243	1.5
SnO_2	0.474	0.237	1.4
SrO	/	0.273	1.6

Table 1. Deposition Parameters of the binary oxides[35–37]

For the SrO-decorated samples, a notable decrease of the factor is observed: 0.5 for $La_{0.9}Sr_{0.1}CoO_{3-\delta}$, and 0.8 for $La_{0.8}Sr_{0.2}CoO_{3-\delta}$ and $La_{0.95}Sr_{0.05}CoO_{3-\delta}$. In contrast, when decorated with CaO, the degradation factor increases, with a factor of 1.6 for $La_{0.9}Sr_{0.1}CoO_{3-\delta}$, 1.4 for $La_{0.95}Sr_{0.05}CoO_{3-\delta}$, and 1.2 for $La_{0.8}Sr_{0.2}CoO_{3-\delta}$. In the case of SnO_2, the decoration leads to a substantial increase in ASR, with a degradation factor of 6.1 for $La_{0.9}Sr_{0.1}CoO_{3-\delta}$, 6.0 for $La_{0.8}Sr_{0.2}CoO_{3-\delta}$, and 4.4 for $La_{0.95}Sr_{0.05}CoO_{3-\delta}$. It is important to note that there are no clear observable trends associated with the Sr content in the $La_{1-x}Sr_xCoO_{3-\delta}$ compositions.

The effect of acceptor dopant concentration in $La_{1-x}Sr_xCoO_{3-\delta}$ on oxygen surface exchange kinetics can be further discussed. Indeed, this study shows no significant influence of the level of Sr nominal concentration of $La_{1-x}Sr_xCoO_{3-\delta}$ on the oxygen surface exchange coefficient. A hypothesis can be formulated to explain this feature. The electronic conductivity at the measured temperature (600 °C) is metallic-type even for the lower Sr concentration[38], *i.e.* 5 at.%. We suggest that the electron concentration at the surface of the $La_{1-x}Sr_xCoO_{3-\delta}$ with the lowest Sr-doping content is high enough not to be limiting for the oxygen exchange reaction. The most noticeable distinction lies in the initial oxygen surface exchange coefficient as shown previously in Figure 2 and Figure 3. This evolution is attributed to the oxygen vacancy concentration of the bulk material. This evolution is still to be clarified considering the rate-limiting step associated is the oxygen adsorption kinetics. As for $La_{0.9}Sr_{0.1}CoO_{3-\delta}$, the peculiar behaviour of the SrO decoration appears to stem from the elevated initial oxygen exchange kinetics of the regenerated electrode.

Next, the impact of decorations on $La_{1-x}Sr_xCoO_{3-\delta}$ compositions is compared with prior findings from Riedl *et al.*[9] on $Pr_{0.1}Ce_{0.9}O_{2-\delta}$.

For the sake of clarity, the relative change of ASR of the different $La_{1-x}Sr_xCoO_{3-\delta}$ samples of this work are averaged and compared with relative change of ASR obtained for $Pr_{0.1}Ce_{0.9}O_{2-\delta}$

Initially, the relative change of ASR values of the pristine samples are depicted alongside the calculated acidity for $Pr_{0.1}Ce_{0.9}O_{2-\delta}$ and an arbitrary value for the three $La_{1-x}Sr_xCoO_{3-\delta}$ compositions of -7.6 considering a more basic surface than CaO (-7.5). Both of the values are represented mainly as a qualitative reference and are not used to contribute to the fitted evolution. Notably, decorations with basic oxides on $Pr_{0.1}Ce_{0.9}O_{2-\delta}$ lead to a substantial reduction in ASR, with SrO and CaO decorations decreasing it by factors of 5.6 and 2.5, respectively, while increasing it by a factor of 3.2 with SnO_2 decoration. The trend for $La_{1-x}Sr_xCoO_{3-\delta}$ appears to be more moderate, with the ASR changing by a factor of 0.69 for SrO decorations and increasing by factors of 1.4 and 5.5 for CaO and SnO_2 decorations, respectively.

Recently Siebenhofer *et al.*[22] formalized a theory on the modifications of surface properties of the electrode with the Smith acidity scale using a combination of experimental data and DFT calculations. As described by Nicollet *et al.*[8] the addition of oxide at the surface of the electrode induce a modification of the work function of the host material. $La_{1-x}Sr_xCoO_{3-\delta}$ exhibits a work function of 4.4 eV while it goes up to 5.1 eV for $Pr_{0.1}Ce_{0.9}O_{2-\delta}$. Then, the decoration of the surface would induce a modification of the ionic potential of the surface creating dipoles. The more basic decorations tend to decrease the work function while more acidic decoration tend to increase the work function. However, this approach does not yet explain the difference of sensitivity of the electrode material to the decoration.

Comparing the evolutions between the two mixed conducting oxides, $Pr_{0.1}Ce_{0.9}O_{2-\delta}$ is more strongly impacted by decorations than the $La_{1-x}Sr_xCoO_{3-\delta}$ compositions. This evolution points toward a surface reaction controlled by the surface acidity. It can be hypothesized that the higher the difference of acidity between the surface and the decoration the more impactful the decoration on the oxygen exchange kinetics will be. This means that, despite its initially bad kinetics, $Pr_{0.1}Ce_{0.9}O_{2-\delta}$ can be improved to a point where its kinetics are closer to the inherently better performing $La_{1-x}Sr_xCoO_{3-\delta}$.

With respect to these observations, although the present study focuses on the effect of decoration at low pO_2 on $La_{1-x}Sr_xCoO_{3-\delta}$ structures, these observations can be considered to hold at higher temperature and higher pO_2 as it was already observed for PCO[8,9] at different pO_2 and temperatures ranges. The effect of work function change extending the effect to other rate-limiting steps.

Finally, with regard to the higher electrochemical stability of $Pr_{0.1}Ce_{0.9}O_{2-\delta}$ due to the lack of cation segregation, these results call for a reassessment of the design principles for solid oxide cell electrodes, focussing on the right combination of surface and host material.

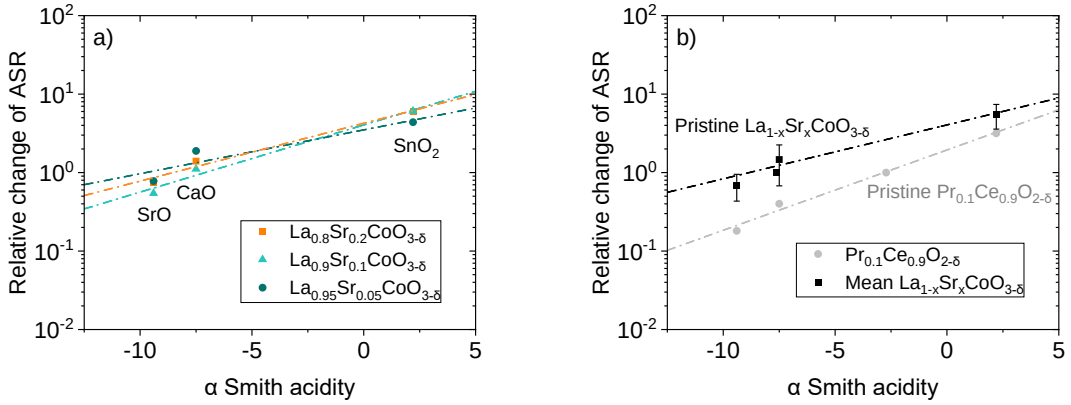

Figure 5. Degradation factor of a) decorated $La_{0.95}Sr_{0.05}CoO_{3-\delta}$ (●), $La_{0.9}Sr_{0.1}CoO_{3-\delta}$ (▲) and $La_{0.8}Sr_{0.2}CoO_{3-\delta}$ (■) and b) mean $La_{1-x}Sr_xCoO_{3-\delta}$ degradation factor (■) compared to the degradation factor of decorated $Pr_{0.1}Ce_{0.9}O_{2-\delta}$ (●) from Riedl et al.[9], evolution with smith acidity of the decoration.

5 Conclusion

The effects of selected impurities (CaO, SrO and SnO_2) at the surface of $La_{1-x}Sr_xCoO_{3-\delta}$ electrodes with various Sr contents were studied by i-PLD measurements. The oxygen exchange kinetics were monitored throughout the decoration process. The temperature dependence between 500 and 600 °C at 0.04 mbar of pO_2 and the pO_2 dependence in the range of 10^{-5} and 10^{-1} bar at 600 °C were studied. It appears that all decorations are detrimental for the oxygen exchange kinetics of the $La_{1-x}Sr_xCoO_{3-\delta}$ electrodes except for a submonolayer decoration with SrO at 600 °C. This observation is independent of the nominal strontium content, which suggests that the effect of decoration is mainly a function of the surface termination of $La_{1-x}Sr_xCoO_{3-\delta}$, and this termination is similar for all compositions.

The effect of impurities changed the performances of the electrodes from an enhancement up to a factor of 2 for SrO decoration to a degradation down to a factor of 6 for SnO_2 decoration at equivalent thickness deposited. Similar to what has been observed previously on $Pr_{0.1}Ce_{0.9}O_{2-\delta}$, the Smith acidity scale appears to serve as a qualitative descriptor for the impact of impurities on the kinetics of oxygen exchange of $La_{1-x}Sr_xCoO_{3-\delta}$.

As the decorations do not change the pO_2 dependence, it seems that the rate-limiting step of the oxygen exchange reaction is not affected by the decoration. However, because the activation energy of the oxygen exchange kinetics is strongly affected by basic decorations, the energy barrier for the rate-limiting step on $La_{1-x}Sr_xCoO_{3-\delta}$ is very sensitive to the decoration, which should be studied further. The change of Sr content in $La_{1-x}Sr_xCoO_{3-\delta}$ showed no clear difference with respect to the decoration impact on oxygen exchange kinetics. As compared with $Pr_{0.1}Ce_{0.9}O_{2-\delta}$ (n-type semi-conductor) from a previous study, $La_{1-x}Sr_xCoO_{3-\delta}$, (metal-like conductor) shows a weaker effect of basic oxide decorations to its exchange kinetics, while acidic oxides are more detrimental than on $Pr_{0.1}Ce_{0.9}O_{2-\delta}$. The effect observed was linked to an acidity difference between the surface and the deposited oxide.

These results have strong implications for future solid oxide cell oxygen electrode design as they emphasize the relative importance of surface and bulk properties of the host oxide. This leads to a high degree of freedom in the choice and combination of materials and opens new opportunities to tailor kinetically fast and electrochemically stable electrodes.

6 Acknowledgment

The authors acknowledge the French national research agency for their financial support through the project ANR-21-CE50-0020.

7 References

(1) Kilner, J. Surface Exchange of Oxygen in Mixed Conducting Perovskite Oxides. *Solid State Ionics* **1996**, *86–88*, 703–709. https://doi.org/10.1016/0167-2738(96)00153-1.

(2) Riedl, C.; Siebenhofer, M.; Nenning, A.; Schmid, A.; Weiss, M.; Rameshan, C.; Limbeck, A.; Kubicek, M.; Opitz, A. K.; Fleig, J. *In Situ* Techniques Reveal the True Capabilities of SOFC Cathode Materials and Their Sudden Degradation Due to Omnipresent Sulfur Trace Impurities. *J. Mater. Chem. A* **2022**, *10* (28), 14838–14848. https://doi.org/10.1039/D2TA03335F.

(3) Tripković, Đ.; Wang, J.; Küngas, R.; Mogensen, M. B.; Yildiz, B.; Hendriksen, P. V. Thermally Controlled Activation and Passivation of Surface Chemistry and Oxygen-Exchange Kinetics on a Perovskite Oxide. *Chem. Mater.* **2022**, *34* (4), 1722–1736. https://doi.org/10.1021/acs.chemmater.1c03901.

(4) Tsvetkov, N.; Lu, Q.; Sun, L.; Crumlin, E. J.; Yildiz, B. Improved Chemical and Electrochemical Stability of Perovskite Oxides with Less Reducible Cations at the Surface. *Nature Mater* **2016**, *15* (9), 1010–1016. https://doi.org/10.1038/nmat4659.

(5) Bucher, E.; Sitte, W.; Klauser, F.; Bertel, E. Impact of Humid Atmospheres on Oxygen Exchange Properties, Surface-near Elemental Composition, and Surface Morphology of $La_{0.6}Sr_{0.4}CoO_{3-\delta}$. *Solid State Ionics* **2012**, *208*, 43–51. https://doi.org/10.1016/j.ssi.2011.12.005.

(6) Bucher, E.; Gspan, C.; Hofer, F.; Sitte, W. Sulphur Poisoning of the SOFC Cathode Material La0.6Sr0.4CoO3-δ. *Solid State Ionics* **2013**, *238*, 15–23. https://doi.org/10.1016/j.ssi.2013.03.007.

(7) Schrödl, N.; Bucher, E.; Egger, A.; Kreiml, P.; Teichert, C.; Höschen, T.; Sitte, W. Long-Term Stability of the IT-SOFC Cathode Materials $La_{0.6}Sr_{0.4}CoO_{3-\delta}$ and $La_2NiO_{4+\delta}$ against Combined Chromium and Silicon Poisoning. *Solid State Ionics* **2015**, *276*, 62–71. https://doi.org/10.1016/j.ssi.2015.03.035.

(8) Nicollet, C.; Toparli, C.; Harrington, G. F.; Defferriere, T.; Yildiz, B.; Tuller, H. L. Acidity of Surface-Infiltrated Binary Oxides as a Sensitive Descriptor of Oxygen Exchange Kinetics in Mixed Conducting Oxides. *Nat Catal* **2020**, *3* (11), 913–920. https://doi.org/10.1038/s41929-020-00520-x.

(9) Riedl, C.; Siebenhofer, M.; Nenning, A.; Wilson, G. E.; Kilner, J.; Rameshan, C.; Limbeck, A.; Opitz, A. K.; Kubicek, M.; Fleig, J. Surface Decorations on Mixed Ionic and Electronic Conductors: Effects on Surface Potential, Defects, and the Oxygen Exchange Kinetics. *ACS Appl. Mater. Interfaces* **2023**, *15* (22), 26787–26798. https://doi.org/10.1021/acsami.3c03952.

(10) Bishop, S. R.; Stefanik, T. S.; Tuller, H. L. Electrical Conductivity and Defect Equilibria of Pr0.1Ce0.9O2−δ. *Phys. Chem. Chem. Phys.* **2011**, *13* (21), 10165. https://doi.org/10.1039/c0cp02920c.

(11) Cao, Y.; Gadre, M. J.; Ngo, A. T.; Adler, S. B.; Morgan, D. D. Factors Controlling Surface Oxygen Exchange in Oxides. *Nat Commun* **2019**, *10* (1), 1346. https://doi.org/10.1038/s41467-019-08674-4.

(12) Lee, Y.-L.; Kleis, J.; Rossmeisl, J.; Shao-Horn, Y.; Morgan, D. Prediction of Solid Oxide Fuel Cell Cathode Activity with First-Principles Descriptors. *Energy Environ. Sci.* **2011**, *4* (10), 3966. https://doi.org/10.1039/c1ee02032c.

(13) Sogaard, M.; Hendriksen, P.; Mogensen, M.; Poulsen, F.; Skou, E. Oxygen Nonstoichiometry and Transport Properties of Strontium Substituted Lanthanum Cobaltite. *Solid State Ionics* **2006**, *177* (37–38), 3285–3296. https://doi.org/10.1016/j.ssi.2006.09.005.

(14) Siebenhofer, M.; Riedl, C.; Nenning, A.; Artner, W.; Rameshan, C.; Opitz, A. K.; Fleig, J.; Kubicek, M. Improving and Degrading the Oxygen Exchange Kinetics of $La_{0.6}Sr_{0.4}CoO_{3-\delta}$ by Sr Decoration. *J. Mater. Chem. A* **2023**, *11* (24), 12827–12836. https://doi.org/10.1039/D2TA09362F.

(15) Siebenhofer, M.; Riedl, C.; Schmid, A.; Limbeck, A.; Opitz, A. K.; Fleig, J.; Kubicek, M. Investigating Oxygen Reduction Pathways on Pristine SOFC Cathode Surfaces by *in Situ* PLD Impedance Spectroscopy. *J. Mater. Chem. A* **2022**, *10* (5), 2305–2319. https://doi.org/10.1039/D1TA07128A.

(16) Rupp, G. M.; Téllez, H.; Druce, J.; Limbeck, A.; Ishihara, T.; Kilner, J.; Fleig, J. Surface Chemistry of $La_{0.6}Sr_{0.4}CoO_{3-\delta}$ Thin Films and Its Impact on the Oxygen Surface Exchange Resistance. *J. Mater. Chem. A* **2015**, *3* (45), 22759–22769. https://doi.org/10.1039/C5TA05279C.

(17) la O', G. J.; Ahn, S.-J.; Crumlin, E.; Orikasa, Y.; Biegalski, M. D.; Christen, H. M.; Shao-Horn, Y. Catalytic Activity Enhancement for Oxygen Reduction on Epitaxial Perovskite Thin Films for Solid-Oxide Fuel Cells. *Angewandte Chemie International Edition* **2010**, *49* (31), 5344–5347. https://doi.org/10.1002/anie.201001922.
(18) Rupp, G. M.; Limbeck, A.; Kubicek, M.; Penn, A.; Stöger-Pollach, M.; Friedbacher, G.; Fleig, J. Correlating Surface Cation Composition and Thin Film Microstructure with the Electrochemical Performance of Lanthanum Strontium Cobaltite (LSC) Electrodes. *J. Mater. Chem. A* **2014**, *2* (19), 7099–7108. https://doi.org/10.1039/C3TA15327D.
(19) Ahamer, C.; Opitz, A. K.; Rupp, G. M.; Fleig, J. Revisiting the Temperature Dependent Ionic Conductivity of Yttria Stabilized Zirconia (YSZ). *J. Electrochem. Soc.* **2017**, *164* (7), F790–F803. https://doi.org/10.1149/2.0641707jes.
(20) Siebenhofer, M.; Huber, T.; Artner, W.; Fleig, J.; Kubicek, M. Substrate Stoichiometry Changes during Pulsed Laser Deposition: A Case Study on SrTiO 3. *Acta Materialia* **2021**, *203*, 116461. https://doi.org/10.1016/j.actamat.2020.10.077.
(21) Fahrnberger, F.; Siebenhofer, M.; Hutter, H.; Kubicek, M. Investigation of Atomic-Scale Decorations on Mixed Conducting Oxides via Time-of-Flight Secondary Ion Mass Spectrometry (ToF-SIMS). *Applied Surface Science* **2023**, *640*, 158312. https://doi.org/10.1016/j.apsusc.2023.158312.
(22) Siebenhofer, M.; Nenning, A.; Rameshan, C.; Blaha, P.; Fleig, J.; Kubicek, M. Engineering Surface Dipoles on Mixed Conducting Oxides with Ultra-Thin Oxide Decoration Layers. *Nat Commun* **2024**, *15* (1), 1730. https://doi.org/10.1038/s41467-024-45824-9.
(23) Joachim Maier. *Physical Chemistry of Ionic Materials: Ions and Electrons in Solids*, John Wiley&Sons.; 2004.
(24) Siebenhofer, M.; Huber, T. M.; Friedbacher, G.; Artner, W.; Fleig, J.; Kubicek, M. Oxygen Exchange Kinetics and Nonstoichiometry of Pristine $La_{0.6}Sr_{0.4}CoO_{3-\delta}$ Thin Films Unaltered by Degradation. *J. Mater. Chem. A* **2020**, *8* (16), 7968–7979. https://doi.org/10.1039/C9TA13020A.
(25) Kawada, T.; Suzuki, J.; Sase, M.; Kaimai, A.; Yashiro, K.; Nigara, Y.; Mizusaki, J.; Kawamura, K.; Yugami, H. Determination of Oxygen Vacancy Concentration in a Thin Film of La0.6Sr0.4CoO3À□ by an Electrochemical Method. *Journal of The Electrochemical Society*.
(26) Souza, R. A. D.; Kilner, J. A. Oxygen Transport in $La_{1-x}Sr_xMn_{1-y}Co_yO_{3-\delta}$ Perovskites. *Solid State Ionics* **1999**.
(27) Gao, R.; Fernandez, A.; Chakraborty, T.; Luo, A.; Pesquera, D.; Das, S.; Velarde, G.; Thoréton, V.; Kilner, J.; Ishihara, T.; Nemšák, S.; Crumlin, E. J.; Ertekin, E.; Martin, L. W. Correlating Surface Crystal Orientation and Gas Kinetics in Perovskite Oxide Electrodes. *Advanced Materials* **2021**, *33* (20), 2100977. https://doi.org/10.1002/adma.202100977.
(28) Nicollet, C.; Tuller, H. L. Perspective on the Relationship between the Acidity of Perovskite Oxides and Their Oxygen Surface Exchange Kinetics. *Chem. Mater.* **2022**, *34* (3), 991–997. https://doi.org/10.1021/acs.chemmater.1c03140.
(29) Chen, X.; Wang, S.; Yang, Y. L.; Smith, L.; Wu, N. J.; Perry, S. S.; Jacobson, A. J.; Ignatiev, A. Electrical Conductivity Relaxation Studies of an Epitaxial $La_{0.5}Sr_{0.5}CoO_{3-\delta}$ Thin Film. *Solid State Ionics* **2002**.
(30) Egger, A.; Bucher, E.; Yang, M.; Sitte, W. Comparison of Oxygen Exchange Kinetics of the IT-SOFC Cathode Materials $La_{0.5}Sr_{0.5}CoO_{3-\delta}$ and $La_{0.6}Sr_{0.4}CoO_{3-\delta}$. *Solid State Ionics* **2012**, *225*, 55–60. https://doi.org/10.1016/j.ssi.2012.02.050.
(31) van der Haar, L. M.; den Otter, M. W.; Morskate, M.; Bouwmeester, H. J. M.; Verweij, H. Chemical Diffusion and Oxygen Surface Transfer of $La_{1-x}Sr_xCoO_{3-\delta}$ Studied with Electrical Conductivity Relaxation. *Journal of The Electrochemical Society* **2002**, *149* (3), J41. https://doi.org/10.1149/1.1446874.
(32) Wang, S.; Kim, G.; Yoon, J. S.; Wang, H.; Huang, D.; Jacobson, A. Electrochemical Properties of Nanocrystalline $La_{0.5}Sr_{0.5}CoO_{3-\delta}$. *Meet. Abstr.* **2009**, *MA2009-01* (5), 290–290. https://doi.org/10.1149/MA2009-01/5/290.
(33) Lee, W.; Han, J. W.; Chen, Y.; Cai, Z.; Yildiz, B. Cation Size Mismatch and Charge Interactions Drive Dopant Segregation at the Surfaces of Manganite Perovskites. *J. Am. Chem. Soc.* **2013**, *135* (21), 7909–7925. https://doi.org/10.1021/ja3125349.

(34) Druce, J.; Téllez, H.; Burriel, M.; Sharp, M. D.; Fawcett, L. J.; Cook, S. N.; McPhail, D. S.; Ishihara, T.; Brongersma, H. H.; Kilner, J. A. Surface Termination and Subsurface Restructuring of Perovskite-Based Solid Oxide Electrode Materials. *Energy Environ. Sci.* **2014**, *7* (11), 3593–3599. https://doi.org/10.1039/C4EE01497A.
(35) Gagnidze, T.; Ma, H.; Cancellieri, C.; Bona, G.-L.; La Mattina, F. Structural Properties of Ultrathin SrO Film Deposited on $SrTiO_3$. *Science and Technology of Advanced Materials* **2019**, *20* (1), 456–463. https://doi.org/10.1080/14686996.2019.1599693.
(36) Kamada, O.; Takizawa, T.; Sakurai, T. A High Temperature X-Ray Diffractometer Using a Solar Furnace. *Japanese Journal of Applied Physics* **1971**, *10* (4), 485. https://doi.org/10.1143/JJAP.10.485.
(37) Semancik, S.; Cavicchi, R. E. The Growth of Thin, Epitaxial SnO_2 Films for Gas Sensing Applications. *Thin Solid Films* **1991**, *206* (1–2), 81–87. https://doi.org/10.1016/0040-6090(91)90397-G.
(38) Mizusaki, J.; Tabuchi, J.; Matsuura, T.; Yamauchi, S.; Fueki, K. Electrical Conductivity and Seebeck Coefficient of Nonstoichiometric $La_{1-x}Sr_xCoO_{3-\delta}$. *J. Electrochem. Soc.* **1989**, *136* (7), 2082–2088. https://doi.org/10.1149/1.2097187.